

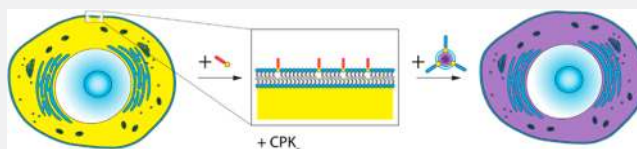
# Drug Delivery via Cell Membrane Fusion Using Lipopeptide Modified Liposomes

Jian Yang,<sup>#</sup> Azadeh Bahreman,<sup>#</sup> Geert Daudey, Jeroen Bussmann, René C. L. Olsthoorn,<sup>\*</sup> and Alexander Kros<sup>\*</sup>

Department of Supramolecular Chemistry & Biomaterials, Leiden Institute of Chemistry, Leiden University, P.O. Box 9502, Leiden, 2300 RA, The Netherlands

## S Supporting Information

**ABSTRACT:** Efficient delivery of drugs to living cells is still a major challenge. Currently, most methods rely on the endocytotic pathway resulting in low delivery efficiency due to limited endosomal escape and/or degradation in lysosomes. Here, we report a new method for direct drug delivery into the cytosol of live cells *in vitro* and *in vivo* utilizing targeted membrane fusion between liposomes and live cells. A pair of complementary coiled-coil lipopeptides was embedded in the lipid bilayer of liposomes and cell membranes respectively, resulting in targeted membrane fusion with concomitant release of liposome encapsulated cargo including fluorescent dyes and the cytotoxic drug doxorubicin. Using a wide spectrum of endocytosis inhibitors and endosome trackers, we demonstrate that the major site of cargo release is at the plasma membrane. This method thus allows for the quick and efficient delivery of drugs and is expected to have many *in vitro*, *ex vivo*, and *in vivo* applications.



## INTRODUCTION

The plasma membrane is the protecting interface between cells and their surrounding environment. Uptake of nutrients occurs through this interface using specialized mechanisms such as endocytosis.<sup>1</sup> Nutrients, or drugs for that matter, are frequently internalized into small transport vesicles called endosomes, which are derived from the cell membrane. For many medicines to become an active drug, they have to enter the cell's cytosol. However, the detrimental environment inside these endosomes can result in degradation of the drug. To date, intracellular delivery of macromolecules is still a major challenge in research and therapeutic applications.<sup>2,3</sup> It is therefore highly desirable to develop new alternative delivery methods that circumvent the endocytosis pathway. So far, all attempts in drug delivery using particles as carriers have been unsuccessful in avoiding this pathway,<sup>4</sup> hence current efforts to develop ways of enhancing endosomal escape.<sup>5</sup>

Cell penetrating peptides (CPPs) have been studied extensively to achieve efficient uptake into the cytosol. However, the current view is that CPPs conjugated to large molecular weight cargo (e.g., liposomes) predominantly are internalized via endocytosis.<sup>6–8</sup> Moreover, the positive charge of CPPs such as the Tat peptide<sup>9</sup> leads to unfavorable interaction with blood components. Other transfection techniques have been devised, such as viral vectors<sup>10</sup> and physical methods.<sup>2,11,12</sup> These methods have their own limitations, including safety issues or their reliance to electrical fields or high pressure.

Fusion of lipid membranes is a vital process in biological systems, facilitating the efficient transport of molecules across membranes.<sup>13–15</sup> *In vivo* membrane fusion shows a broad

variety, from synaptic to viral and extracellular fusion, and was found to be a highly regulated process, specific in time and place, which is achieved by a complex interplay of different functional proteins.<sup>16</sup> For example, in the process of neuronal exocytosis, docking of transport vesicles to the target plasma membrane is mediated by the coiled-coil formation of complementary SNARE protein subunits on the opposing membranes.<sup>17</sup> This forces the opposing membranes into close proximity, resulting ultimately in lipid mixing followed by pore formation and concomitant content transfer.

As a bottom-up approach, several synthetic models systems have been developed to mimic membrane fusion events, but in general these simple systems do not always recapitulate the basic characteristics of native membrane fusion.<sup>18–22</sup> Furthermore, all these approaches were limited to liposome–liposome fusion studies and have not shown to induce fusion events in live cells, thereby limiting their use for future drug delivery purposes.

Inspired by the SNARE protein complex, our laboratory has developed a fully artificial membrane fusion system composed of a complementary pair of lipidated coiled-coil peptides enabling targeted liposome–liposome fusion.<sup>23</sup> This model system possesses all the key characteristics of targeted membrane fusion similar to SNARE mediated fusion including lipid and content mixing in the absence of leakage (Figure 1A–B).<sup>24,25</sup> In our membrane fusion system, coiled-coil forming peptides “E<sub>3</sub>” [(EIAALEK)<sub>3</sub>] and “K<sub>3</sub>” [(KIAALKE)<sub>3</sub>] were conjugated to a cholesterol moiety via a polyethylene glycol

Received: June 14, 2016

Published: August 22, 2016

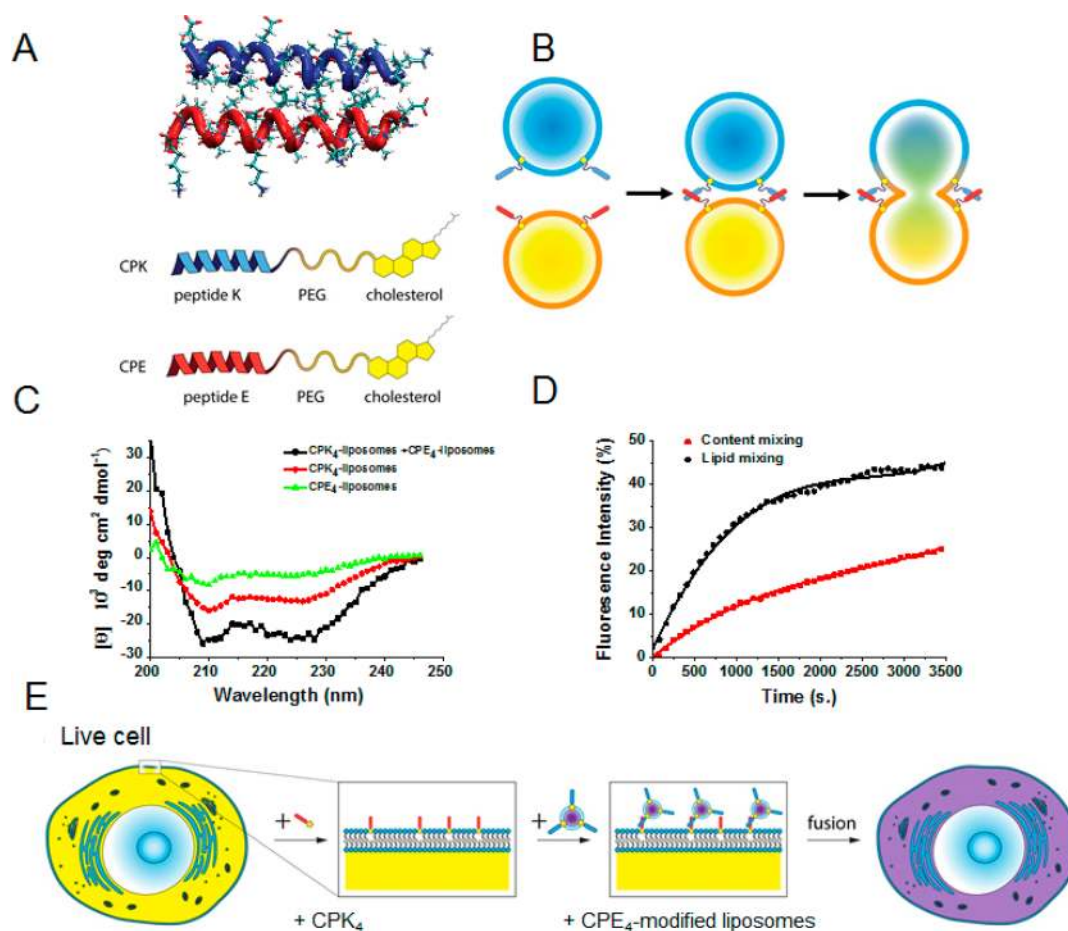


**Figure 1.** Schematic representation of (A) coiled-coil structure between peptides E and K (adapted from PDB 1UO1), (B) targeted liposome fusion mediated by coiled-coil formation between CPE<sub>4</sub> modified liposomes and CPK<sub>4</sub> modified liposomes, (C) CD spectra of CPE<sub>4</sub> modified liposomes, and CPK<sub>4</sub> modified liposomes and an equimolar mixture thereof. The total lipid concentrations were 0.5 mM with 1 mol % of lipidated peptide in PBS. (D) Lipid mixing and content mixing between CPE<sub>4</sub>-liposomes and CPK<sub>4</sub>-liposomes. Fluorescence traces showing lipid mixing between E and K decorated liposomes, as measured through an increase in NBD fluorescence. Total lipid concentrations were 0.1 mM with 1 mol % of lipidated peptide, in PBS; fluorescence graphs indicating content mixing between sulphorhodamine loaded (20 mM), CPE<sub>4</sub> decorated liposomes and nonfluorescent, CPK<sub>4</sub> decorated liposomes. Total lipid concentrations were 0.25 mM with 1 mol % lipidated peptide in PBS. (E) Scheme of fusion between cell and liposomes.

(PEG) spacer, yielding lipopeptides CPE<sub>3</sub> and CPK<sub>3</sub>. The cholesterol moiety allows for the immediate insertion of the lipidated peptides into any phospholipid membrane. We demonstrated that plain membranes could become fusogenic by the spontaneous insertion of CPE<sub>3</sub> and CPK<sub>3</sub> in the bilayer. A follow-up study showed that CPK<sub>3</sub> modified cells and zebrafish embryos could be specifically labeled with the complementary fluorescently labeled E<sub>3</sub> peptide,<sup>23</sup> revealing that E<sub>3</sub>/K<sub>3</sub> coiled-coil formation is also functional in an *in vivo* environment, thereby paving the way for targeted delivery using peptide modified liposomes.

Here, we report a new drug delivery method based on targeted membrane fusion between liposomes and live cells. We demonstrate that a wide range of cell lines can be specifically modified with lipopeptide CPK<sub>4</sub>, and upon addition of CPE<sub>4</sub> decorated liposomes membrane fusion occurs with concomitant efficient cytosolic delivery of a variety of compounds such as fluorescent dyes propidium iodide (PI), TOPRO3, and the cytotoxic drug doxorubicin (DOX). The mechanism of content uptake was studied using endocytosis inhibitors and endosome trackers in order to prove that the major site of cargo release into the cells is indeed at the plasma membrane due to

liposome-cell fusion. Additionally, we show cytosolic dye (and drug) delivery *in vivo* using zebrafish embryos. Our method thus allows for quick and efficient delivery of drugs and bio(macromolecules) without cell damage and is expected to have many applications *in vitro*, *ex vivo*, and *in vivo*.

## RESULTS AND DISCUSSION

### Coiled-Coil Formation between CPE<sub>4</sub> and CPK<sub>4</sub>.

Previously, we reported docking of liposomes at cell membranes using peptides CPE<sub>3</sub> and CPK<sub>3</sub>, but membrane fusion was not observed.<sup>23</sup> In the present study we increased the number of heptad repeats in CPE and CPK to four thereby enhancing coiled-coil stability,<sup>26</sup> expecting that this would favor liposome-cell fusion. Figure 1C shows that the cholesterol- and PEG-modified E<sub>4</sub> and K<sub>4</sub>—hereafter called lipopeptides CPE<sub>4</sub> and CPK<sub>4</sub>—when attached to liposomes, are capable of coiled-coil formation as evident from circular dichroism (CD) spectroscopy, in agreement with previous experiments using CPE<sub>3</sub> and CPK<sub>3</sub>. Next, lipid mixing experiments were performed to investigate the fusogenicity of the CPE<sub>4</sub>/CPK<sub>4</sub> pair in a liposome–liposome assay. In these experiments a fluorescence resonance energy transfer (FRET)-pair consisting

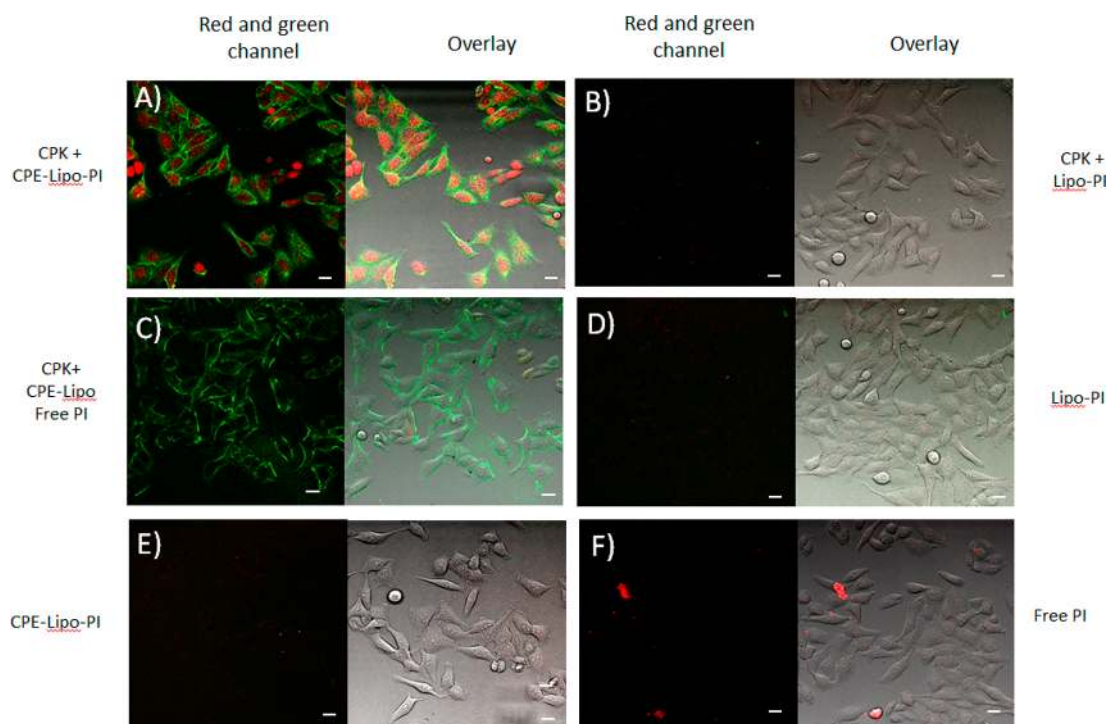


**Figure 2.** Delivery of PI by peptidated-liposomes is dependent on coiled-coil formation between CPK and CPE. Confocal microscopy images of HeLa cells. Cells were preincubated with CPK (A, B, C) or medium (D, E, F) for 2 h, followed by treatment with CPE-decorated liposomes containing PI (A, E), liposomes containing PI (B, D), CPE-decorated liposomes plus free PI (C), or free PI (F). Green: NBD, red: PI. Scale bar is 25  $\mu\text{m}$ . Overlay is red and green channel plus bright field image.

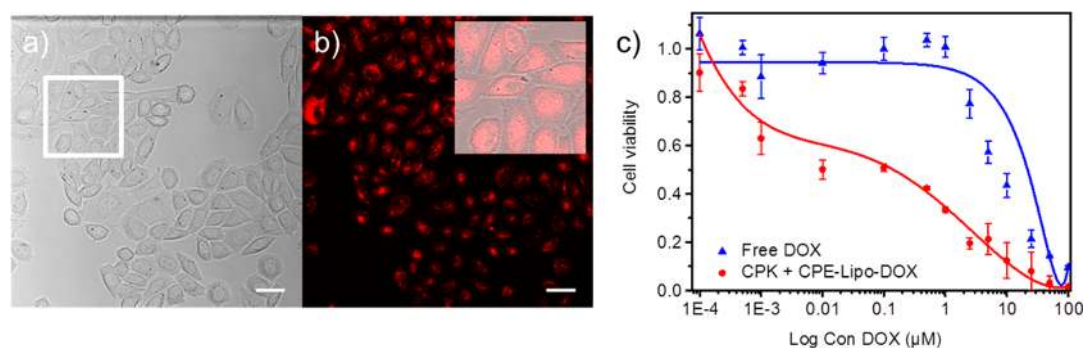
of nitrobenzoxadiazole (NBD) and lissamine rhodamine (LR) fluorophore labeled lipids was incorporated into the membrane of CPK-decorated liposomes.<sup>21</sup> Upon lipid mixing of the latter liposomes with CPE<sub>4</sub>-liposomes the distance between NBD and LR increased, resulting in increased NBD-fluorescence as shown in Figure 1D. Content mixing was quantified by incorporating a sulforhodamine B at a self-quenching concentration of 20 mM into CPE-decorated liposomes and mixing these with CPK-liposomes as described.<sup>23</sup> The increase in sulforhodamine B fluorescence over time indicated that full fusion took place between CPE<sub>4</sub> and CPK<sub>4</sub>-liposomes (Figure 1D). Control experiments verified that the increase in sulforhodamine B fluorescence was not caused by leakage during fusion (Supplementary Figure 1).

#### Coiled-Coil Formation Triggers Liposome-Cell Fusion.

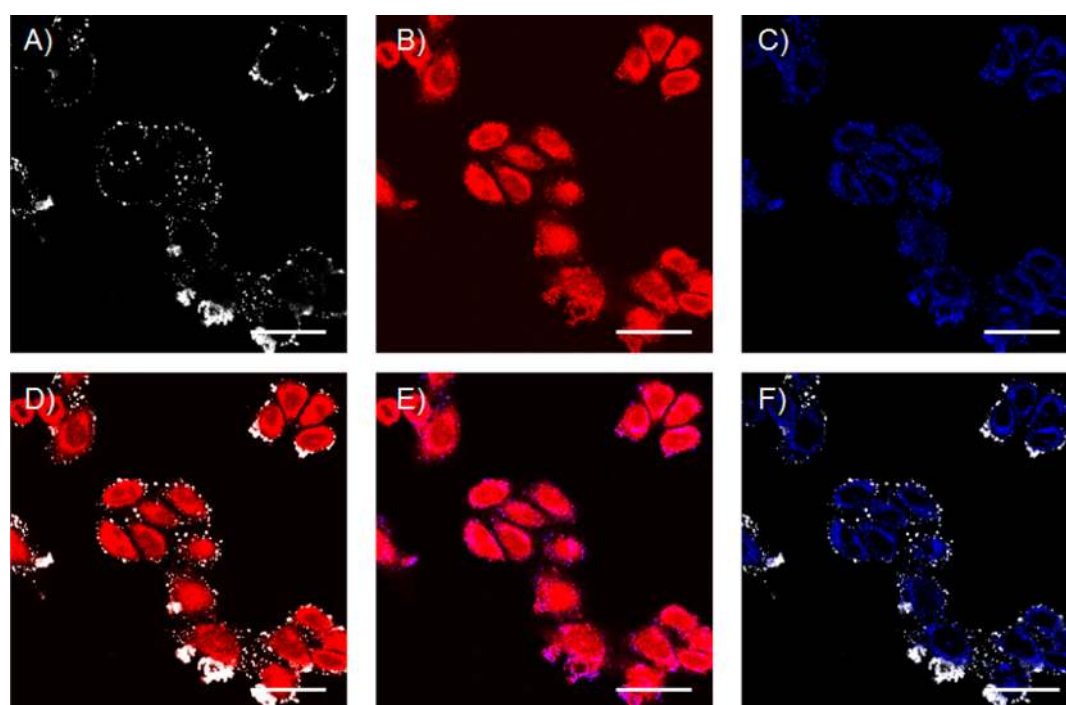
Next we investigated whether CPE<sub>4</sub> and CPK<sub>4</sub> could also mediate membrane fusion between liposomes and living cells. To this end, HeLa cells were preincubated with a micellar solution of CPK<sub>4</sub> for 0.5–2 h before CPE<sub>4</sub>-decorated liposomes (lipid composition DOPC/DOPE/CH, 50:25:25 mol %) containing the nucleic acid stain propidium iodide (PI) or TOPRO3 in their aqueous interior were added as schematically shown in Figure 1E. In order to localize the lipid bilayer, these liposomes also contained 1 mol % of green-fluorescent NBD-DOPE lipids. As expected, confocal microscopy showed that cell membranes became labeled with the green NBD-dye on their outside in line with previous studies.<sup>23</sup> Strikingly, the red dye was observed in the cytosol and nucleus, indicating that membrane fusion and content release had occurred (Figure 2A and Supplementary Figure 2A for TOPRO). Control experiments in which one of the two lipopeptides was omitted showed neither uptake of PI or TOPRO3 nor NBD-labeling of the cell plasma membrane (Figure 2B,C,E and Supplementary

Figure 2). We note that when CPK-treated cells were incubated with empty CPE<sub>4</sub>-decorated liposomes in the presence of free dye only a weak fluorescent signal was observed inside cells (Figure 2C and Supplementary Figure 2C). This control experiment rules out the possibility that residual non-encapsulated dye in our liposome preparation entered the cell by transient membrane destabilization during fusion events. Finally cell incubation with free dyes also did not show any signal of the dye inside the cells (Figure 2F and Supplementary Figure 2F). Similar to CPE<sub>4</sub> decorated liposomes, we also used CPK<sub>4</sub> decorated liposomes containing PI and incubated these with CPE<sub>4</sub> pretreated HeLa cells. However, the delivery of PI was less efficient. A reason might be the asymmetric nature of the fusion system. It was recently shown that peptide E does not interact with a membrane. In contrast, peptide K does interact with the membrane in a so-called snorkeling mode, and this peptide–membrane interaction is in equilibrium with either peptide K homocoiling or E/K coiled-coil formation.<sup>27,28</sup> These studies suggest that peptide K-membrane interactions result in increased membrane curvature supporting membrane fusion. A cell membrane is more complex in composition and therefore less susceptible to undergo fusion as compared to the fusogenic liposomes (DOPC/DOPE/CH 2:1:1) used in this study. Our current thought is that peptide K needs to be on the cell membrane prior to a fusion event in order to activate the complex cell membrane by inducing membrane curvature.<sup>29</sup> However, more studies are required to support this hypothesis.

To exclude the possibility that peptide-mediated liposomal dye delivery was a peculiarity of HeLa cells, the membrane fusion experiments were repeated with Chinese hamster ovary (CHO) and mouse fibroblast (NIH/3T3) cell lines. Again the appearance of TOPRO3 and PI was observed inside cells suggesting that the peptide-mediated delivery of the dye is cell



**Figure 3.** Delivery of DOX into HeLa cells. (a) CPE/CPK mediated delivery of DOX into HeLa cells. Cells were treated with CPK for 1 h followed by incubation with 0.25 mM CPE-liposomes containing with DOX for 15 min. Images were taken after washing. (a) Bright field. (b) Fluorescence channel. The inset shows a magnified overlay image, revealing the presence of DOX in the nucleus. The concentration of DOX loaded into liposomes is 5  $\mu\text{M}$ . Scale bar represents 25  $\mu\text{m}$ . (c) Cytotoxicity of CPE/CPK delivered DOX and free DOX. HeLa cells were treated with CPK for 1 h and series of concentrations of CPE decorated liposomes containing DOX (blue line), or the same concentrations of free DOX (red line) for 12 h. After washing and incubation with medium for 24 h, cell viability was measured by a WST-1 assay.



**Figure 4.** Visualization of endosomes using an endosome tracker. CHO cells were treated with CPK for 2 h, followed by coincubation with pHrodo red dextran and CPE-decorated liposomes (0.25 mM total lipid concentration and 1 mol % CPE) loaded with TOPRO 3. (A) White channel showing DOPE-NBD liposomes. (B) Red channel (TOPRO3). (C) Blue channel (pHrodo). (D) Overlay of panels A and B. (E) Overlay of panels B and C. (F) Overlay of panels A and C. Scale bar is 25  $\mu\text{m}$ .

type independent (Supplementary Figures 3 and 4). Importantly, we found that uveal melanoma cells (Mel270), which are generally hard to transfect,<sup>30,31</sup> could also be modified with TOPRO3 using this method (Supplementary Figure 3D).

To address the potential toxicity of CPK<sub>4</sub>, CPE<sub>4</sub>, and liposomes toward CHO, NIH/3T3, and HeLa cells cell viability assays were carried out. These assays indicated that lipopeptides CPE<sub>4</sub> and CPK<sub>4</sub> and liposomes, with or without CPE<sub>4</sub>, at the concentrations used throughout this study are well tolerated by all cell lines (Supplementary Figure 5A). Higher concentrations of these lipopeptides, even up to 100  $\mu\text{M}$ , did not significantly reduce cell viability when exposed for 2 h but only did so after 24 h of exposure (Supplementary Figure 5B,C).

Altogether, these results show that coiled-coil formation between CPK<sub>4</sub> and CPE<sub>4</sub> is critical for fusion and release of the dyes and that these compounds are not toxic for living cells at the concentrations used allowing to investigate potential applications and their uptake mechanism.

**Delivery of Doxorubicin.** Doxorubicin (DOX) is one of the mostly used drugs for cancer treatments in the clinic today but as a free drug has serious cardiotoxicity. DOX is a cell-permeable drug whose fluorescence is strongly enhanced upon binding to nucleic acids. Intercalation into DNA ultimately results in apoptosis.<sup>32</sup> To test delivery of liposomal DOX, HeLa cells were preincubated with CPK<sub>4</sub> and subsequently exposed to CPE<sub>4</sub>-decorated liposomes containing 5  $\mu\text{M}$  DOX for 15 min. As can be seen in Figure 3a,b this resulted in strong nuclear (and cytosolic) fluorescence. Control experiments

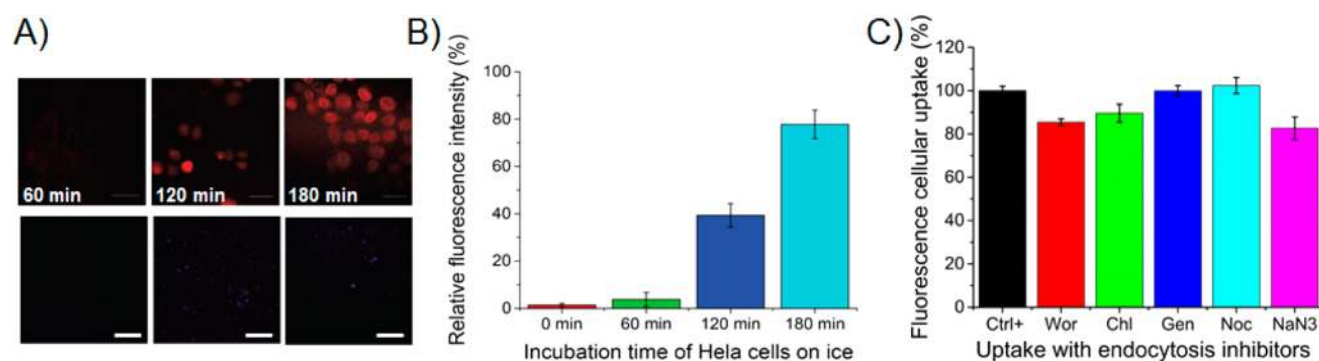


**Figure 5.** Investigation into the uptake mechanism. (A) Effect of low temperature incubation of HeLa cells on liposomal delivery of TOPPRO3 and endosomal uptake of pHrodo. Cells were preincubated on ice with  $5 \mu\text{M}$  CPK (2 h), followed by 15 min incubation with  $0.25 \text{ mM}$  CPE-decorated liposomes containing TOPPRO3. After three washes confocal images were taken immediately (0 min) and after 60, 120, and 180 min. Top row: TOPPRO3 (red), bottom row: pHrodo (blue). (B) Graphical representation of the percentage of TOPPRO dye uptake by HeLa cells on ice. Fluorescence intensities were calculated by ImageJ and plotted as a percentage relative to the fluorescence of TOPPRO3 delivery at  $37^\circ\text{C}$  (100%). Scale bar is  $25 \mu\text{m}$ . (C) Effect of endocytosis and macropinocytosis inhibitors on delivery of PI by liposomes to HeLa cells. Cells were incubated with medium (Ctrl+), or medium containing  $0.25 \mu\text{M}$  wortmannin (Wor),  $40 \mu\text{M}$  chlorpromazine (Chl),  $200 \mu\text{M}$  genistein (Gen),  $40 \mu\text{M}$  nocodazole (Noc) for 1 h,  $0.01\%$  w/v sodium azide (NaN3), followed by 2 h incubation with  $5 \mu\text{M}$  CPK in the presence of inhibitors, and then treated for 15 min with CPE-liposomes containing PI. Final concentration of lipids (liposomes) was  $0.25 \text{ mM}$ . Cellular uptake was measured by flow cytometry. Positive control (100%): fluorescence of PI dye in the absence of inhibitors.

showed that DOX delivery is highly dependent on the presence of CPE<sub>4</sub> and CPK<sub>4</sub> (Supplementary Figure 6). To investigate cytotoxicity of liposomal delivered DOX, HeLa cells preincubated with CPK were exposed with increasing concentrations of DOX-loaded liposomes for 12 h. Cell viability was measured 24 h later. Figure 3c shows cell viability as a function of liposomal and free DOX. As expected, very low concentrations of free DOX ( $<1 \mu\text{M}$ ) did not affect the viability of HeLa cells as passive crossing into cells is not efficient at this concentration. Importantly, in current treatments in the clinic the DOX concentration is up to  $9 \mu\text{M}$  in the serum of patients. In contrast, liposomes loaded with  $1 \mu\text{M}$  Dox did show a significant effect as the DOX uptake is significantly enhanced. Liposomally delivered DOX reduced cell viability at DOX concentrations as low as  $0.1 \text{ nM}$  with an  $\text{IC}_{50}$  of  $\sim 0.01 \mu\text{M}$ , while free DOX did not affect cell viability at concentrations up to  $1 \mu\text{M}$  ( $\text{IC}_{50} \sim 5 \mu\text{M}$ ). Control experiments in which either CPK<sub>4</sub> or CPE<sub>4</sub> was omitted showed 100-fold or higher  $\text{IC}_{50}$  values (Supplementary Figure 7). Thus, our peptide-mediated delivery of DOX can potentially reduce the dose of DOX needed for anticancer treatments thereby lowering the cardiotoxicity of DOX.<sup>33</sup> The presented fusion mediated delivery approach is also promising for the delivery of other drugs or biomolecules like DNA or siRNA.

**Liposomes and Content Only Partially Colocalize with Endosomes.** Endocytosis is the most common pathway for the uptake of small particles including liposomes by cells.<sup>4</sup> To investigate whether endocytosis played a role in the liposomal delivery, the endosome tracker pHrodo, a fluorescently labeled dextran, was used in combination with TOPPRO3 loaded liposomes. TOPPRO3 was chosen as encapsulated dye for this experiment instead of PI because its emission (Ex/Em 642/661 nm) is expected not to interfere with emission of pHrodo (Ex/Em 560/585 nm) making investigation of colocalization of dyes easier. pHrodo and CPE-decorated liposomes containing 1 mol % NBD-DOPE and TOPPRO3 were simultaneously added to CPK-modified HeLa cells. Confocal microscopy showed the presence of TOPPRO3 in the cytosol and to a lesser extent in the nucleus (Figure 4B), while pHrodo was mainly observed as individual dots in the cytosol in agreement with its endosomal

uptake (Figure 4C). Overlaying the fluorescent images of TOPPRO3 and pHrodo revealed some overlap between TOPPRO3 and endosomes (Figure 4E, pink dots), but the majority of TOPPRO3 signal remains unmixed. Again, the signal from NBD-DOPE (Figure 4A, white dots) remained at the plasma membrane, although some overlap with pHrodo was observed at the plasma membrane (Figure 4F). This could be the result of both liposomes and endosome tracker binding at a common spot at the plasma membrane or could mean that some liposomes are initially taken up by endocytosis but then rapidly fuse with the endosomal membrane.

These results suggest that the endosomal uptake pathway only plays a minor role in CPE<sub>4</sub>–CPK<sub>4</sub> mediated liposomal uptake and that liposome-cell membrane fusion is the main route for cargo delivery. This is also illustrated by performing the same experiment at  $4^\circ\text{C}$ , conditions under which active uptake by endocytosis is inhibited. Imaging of cells over a period of 3 h showed the increasing uptake of TOPPRO3 (Figure 5A, upper panels). In contrast only a faint signal of endosome tracker pHrodo was observed after 3 h, indicating that endocytosis was severely limited at  $4^\circ\text{C}$  (Figure 5A, lower panels). Quantification of the fluorescence intensity using software (ImageJ) showed that after 3 h the uptake of TOPPRO3 reached  $\sim 80\%$  of the level obtained after 30 min at  $37^\circ\text{C}$  (Figure 5B). The slower uptake is presumably caused by the reduced rate of liposome-cell fusion events at  $4^\circ\text{C}$ . This is supported by the observation that liposome-liposome lipid mixing induced by CPE<sub>4</sub>/CPK<sub>4</sub> is also significantly slower at  $4^\circ\text{C}$  than at room temperature (Supplementary Figure 8).

**Endocytosis and Macropinocytosis Inhibitors Marginally Affect Delivery.** As independent support for our conclusion that fusion at the plasma membrane is the major pathway for our liposome-based delivery system, several well-characterized inhibitors of endocytotic pathways were tested using flow cytometry measurements and confocal microscopy imaging. Wortmannin blocks PI3-kinase and inhibits macropinocytosis,<sup>34–37</sup> chlorpromazine interferes with clathrin-dependent endocytosis,<sup>38–40</sup> genistein inhibits tyrosine-phosphorylation of Cav 1 and caveola-dependent endocytosis.<sup>41–43</sup> In addition, nocodazole, an inhibitor of microtubule formation,

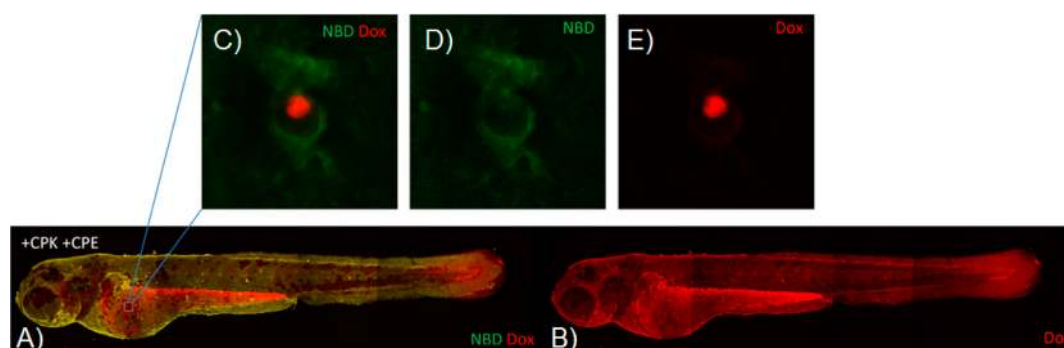


**Figure 6.** In vivo delivery of DOX using CPK and CPE. 2 dpf zebrafish were treated with CPK for 30 min, followed by 30 min incubation with CPE-decorated liposomes (0.25 mM total lipid concentration and 1 mol % CPE) loaded with DOX. (A, B) Whole-embryo imaging showing widespread DOX delivery in living zebrafish embryos (control experiments in [Supplementary Figure S9](#)). (C–E) Single zebrafish skin epithelial cell (from the indicated site of the embryo in (A, B) displaying membrane associated DOPE-NBD labeling (NBD) and predominantly nuclear DOX labeling.

was used to investigate whether intracellular trafficking and internalization mechanisms are involved.<sup>36,37,40,44,45</sup> Moreover, endocytosis of nanoparticles is an energy-dependent mechanism. Sodium azide was therefore used to deplete the energy needs for endocytosis and restrict metabolic activity.<sup>46,47</sup>

HeLa cells were first incubated for 1 h with each inhibitor at concentrations that have been reported by others to show optimal activity. After removal of the inhibitors, cells were treated with CPK and subsequently with CPE-decorated liposomes containing PI dye in the presence of freshly added inhibitors. FACS analysis showed that genistein and nocodazole had no adverse effect on the delivery of PI ([Figure 5C](#)), whereas in the presence of wortmannin, chlorpromazine and sodium azide PI uptake was reduced less than 20%. These results argue against a major role of endocytosis or pinocytosis in uptake of liposomal cargo and support that the dominant pathway for delivery is indeed targeted membrane fusion between liposomes with the plasma membrane of live cells.

**Intracellular Delivery *in Vivo*.** As a first step toward clinical application, we used zebrafish embryos to evaluate direct cytoplasmic delivery *in vivo*. We previously established coiled-coil mediated docking of liposomes onto the zebrafish embryonic skin.<sup>21</sup> During embryonic stages, the zebrafish skin is composed of a layer of ridged, mucus-covered enveloping layer (EVL) cells. Through interspersed gaps in the EVL layer, cells within the underlying epidermal basal layer (EBL), including mucus-secreting cells and ionocytes, are exposed to the external environment.<sup>45</sup> To test for *in vivo* delivery to skin epithelial cells, we exposed 48-h-old zebrafish embryos to CPK in embryo medium for 30 min. After washing, embryos were exposed to NBD-labeled, CPE-decorated liposomes containing DOX for 30 min. Consistent with previous results,<sup>21</sup> we observed widespread liposome docking after 30 min of incubation, as evidenced by NBD and DOX colabeling. Importantly, we identified nuclear DOX labeling within a subset of skin epithelial cells ([Figure 6](#)) consistent with delivery into EBL-layer, but not EVL layer cells, which appeared to be inaccessible due to mucus covering or membrane ridging. Control experiments established that cytoplasmic delivery was specific to coiled-coil interaction ([Supplementary Figure 9](#)). We further confirmed intracellular delivery using liposomes loaded with PI, which becomes highly fluorescent only after interaction with cellular DNA or RNA ([Supplementary Figures 10 and 11](#)). Together, these results indicate the potential application of coiled-coil induced membrane fusion for direct cellular drug delivery *in vivo*.

## CONCLUSIONS

Numerous methods exist to deliver drugs and (bio)-macromolecules to living cells. Depending on the nature of these molecules they can be delivered into cells via electroporation, microinjection, calcium phosphate coprecipitation, nanoparticles, or viral particles. However, many of these methods are either not suitable for *in vitro* use or cannot be safely applied in *in vivo* applications, or are inefficient due to endosomal entrapment and degradation. The membrane fusion system described here involves the targeted fusion of liposomes with the plasma membrane of live cells. As a result, endosomal pathways are almost completely circumvented, and therefore this efficient drug delivery method is suited for labile (bio)molecules. In addition, the lipopeptides and modified liposomes have a low toxicity at the used concentration—in contrast to CPP-based delivery approaches or PEG-induced liposome fusion.<sup>48</sup> We anticipate that this membrane fusion strategy will spark new *in vitro*, *ex vivo* research in the field of chemical biology and possibly in long term *in vivo* applications, enabling new basic and applied research studies for gene therapy. Moreover any compound that can be encapsulated in liposomes like hydrophilic low molecular weight drugs<sup>49</sup> or DNA/siRNA<sup>50,51</sup> could be considered as well as many hydrophilic drugs are unable to enter cells effectively and are known to be degraded in a lysosomal environment thereby lowering their therapeutic efficacy.<sup>52</sup> Here, fusion mediated delivery could result in less degradation of sensitive molecules and might therefore find use as a new transfection agent in *in vitro* cell studies. Also lipid bilayer-coated nanoparticles<sup>53–57</sup> might be delivered more efficiently when coiled-coil mediated membrane fusion is applied thereby increasing the scope of molecules and nanoparticles/nanomedicines that can be delivered into cells. Future *in vivo* application of this technique requires cells to be premodified with one of the two peptides and is currently not cell-type specific due to the cholesterol-anchor; several applications are still conceivable. These include topical administration of drugs to treat, e.g., pulmonary disease or combat respiratory infections like influenza. On the other hand, delivery of liposomally encapsulated mRNA or DNA coding for the tumor suppressor p53 will only affect tumor cells and leave healthy cells unharmed.<sup>58</sup> Similarly, liposomal delivery of miRNA or siRNA to upregulate tumor suppressors or downregulate oncogenes could selectively kill only tumor cells.<sup>59</sup>

Finally, a certain degree of selectivity can be achieved using a light-induced membrane fusion system that was recently developed in our laboratory. This system makes use of photoinduced deshielding of a PEGylated CPE and thus allows potentially for spatiotemporal control of liposomal drug delivery in vivo.<sup>60</sup>

## MATERIALS AND METHODS

Fmoc-protected amino acids were purchased from Novabiochem, and Biosolve Sieber Amide resin was purchased from Chem-Impex International and Agilent Technologies. DOPE, DOPC, DOPE-NBD, and DOPE-LR were purchased from Avanti Polar Lipids. Cholesterol, propidium iodide (#BCBM1455V), and sulphorhodamine were obtained from Sigma-Aldrich. Topro3-Iodide (#1301286) and pHrodo Red dextran 10,000MW were purchased from Life Technologies. Eight wells slide Lab-tek was purchased from Thermo Scientific, USA. DMEM medium was obtained from Gibco, life technologies. N<sub>3</sub>-PEG<sub>4</sub>-COOH<sup>61</sup> and 3-azido-5-cholestene<sup>62</sup> were synthesized following literature procedures.

**Lipopeptide Synthesis and Purification.** The peptide components of CPK<sub>4</sub> and CPE<sub>4</sub>, i.e., E<sub>4</sub> (EIAALEK)<sub>4</sub> and K<sub>4</sub> (KIAALKE)<sub>4</sub>, were synthesized on an automatic CEM peptide synthesizer on a 250 μmol scale using Fmoc chemistry and standard solid-phase peptide synthesis protocols as previously described.<sup>23</sup> After Fmoc deprotection N<sub>3</sub>-(ethylene glycol)<sub>4</sub>-COOH was coupled to the peptide on the resin. After azide reduction cholesteryl-4-amino-4-oxobutanoic acid was coupled to the PEG<sub>4</sub> linker to yield the CPE<sub>4</sub> and CPK<sub>4</sub> peptides as described. The final products were purified by HPLC using a C4 column, and their identity was confirmed by LC-MS.

**Liposome Preparation and Characterization.** Lipids were dissolved in CHCl<sub>3</sub> in the molar ratio DOPC, DOPE, cholesterol, and DOPE-NBD of 49.5:24.75:24.75:1 [total lipid concentration] = 1 mM. Peptide stock solutions of 50 μM were prepared in CHCl<sub>3</sub>/CH<sub>3</sub>OH (1:1 v/v). Liposomes were prepared by mixing the appropriate amount of lipids and CPE<sub>4</sub> in a 20 mL glass vial and evaporating the solvents over air pressure to form lipid films. Traces of solvent were removed under high vacuum for 3–4 h at 25 °C. Each sample was then hydrated with 15 mM PI (Sigma Aldrich #BCBM1455V) or 0.25 mM Topro3 (Life Technologies, #1301286, after removing DMSO by freeze-drying) or FITC-dextran (35 mg/mL) in PBS buffer and sonicated for 2–3 min in a sonication bath at 55 °C. Nonencapsulated dyes or FITC-dextran were removed via Sephadex G25 or G50 size-exclusion PD-10 Columns (GE-Healthcare, USA). Liposomes were characterized by dynamic light scattering (DLS) at 25 °C to determine the average diameter (80–100 nm in general). The final concentration of lipids and CPE<sub>4</sub> in each sample before cell treatments was 250 μM and 2.5 μM, respectively.

Doxorubicin (DOX) was entrapped as follows. The lipid film was hydrated with citrate buffer (pH 3.5) and sonicated in a sonication bath at 50 °C for 30 min. The citrate buffer was replaced by PBS (pH 7.4) through Sephadex G-25 filtration, leaving the inside of liposomes acidic. Doxorubicin powder (Sigma Aldrich #44538) was added into liposomal dispersion at a drug-to-lipid molar ratio of 1:3 and subsequently rotated at 4 °C overnight. Untrapped free DOX was separated from liposomes by size exclusion chromatography using a Sephadex G-25 column. The entrapment efficiency was determined using UV-vis spectrophotometry (see [Supporting Information](#)).

Liposomes obtained were ~120 nm in diameter with a PDI of <0.2.

A CPK<sub>4</sub> stock solution (50 μM) was prepared in CHCl<sub>3</sub>/CH<sub>3</sub>OH (1:1). For a typical cell treatment the appropriate amount of CPK stock solution was taken, and the organic solvent was evaporated under air stream. After that it was hydrated by DMEM (± FCS, w/o phenol red) and sonicated at 55 °C for 1–2 min.

**Cellular Uptake Assay and Confocal Microscopy Measurements.** All incubations were done in complete medium without phenol red. Cells were grown in an 8-well slide at a density of 2.5 × 10<sup>4</sup> cells per well and incubated at 37 °C in 7% CO<sub>2</sub> atmosphere. After 21 h, medium was removed and a CPK<sub>4</sub> solution (5 μM) in medium was added and incubated for 0.5–2 h at 37 °C in 7% CO<sub>2</sub>. After removal of CPK<sub>4</sub>, cells were washed with medium and incubated with CPE<sub>4</sub>-decorated liposomes (250 μM) containing NBD, PI, TOPRO3. After 15 min incubation, cells were washed three times with medium, and fluorescent images were acquired on Leica TCS SP8 confocal laser scanning microscope. Leica application suite advanced fluorescence software (LAS AF, Leica Microsystems B.V., Rijswijk, The Netherlands) and ImageJ (developed by the National Institutes of Health) were used for image analysis and liposome colocalization studies. Wavelength settings for pHrodo Red dextran were Ex/Em: 560/585 nm (Ex laser: 488 nm), for Topro3 Ex/Em: 641/662 nm (Ex laser: 633 nm), for propidium iodide Ex/Em: 535/617 nm (Ex laser: 543 nm), for NBD-DOPE Ex/Em: 455/530 nm (Ex laser: 488 nm) and for DOX Ex/Em: 490/590 nm (Ex laser: 543 nm).

When performing cellular uptake assays on ice, an 8-well slide was placed on ice for 1 h, before adding CPK<sub>4</sub>. After 2 h on ice, CPK<sub>4</sub> was removed and after washing CPE<sub>4</sub>-decorated liposomes loaded with TOPRO3 and endosome tracker were added simultaneously. After 15 min incubation on ice, cells were washed three times with ice-cold medium and imaged immediately (time point 0 h). After 1, 2, and 3 h the slide was transferred to the microscope and images were recorded. In between measurements the cells were kept on ice.

**Cell Viability Assay.** Cells were seeded in a 96 well-plate at a concentration of 1 × 10<sup>4</sup> cells per well and incubated for 24 h prior to the WST-1 assay. The medium was removed, and cells were incubated with 100 μL of CPK<sub>4</sub> (5 μM) solution in medium (w/o phenol red) for 2 h. After 2 h CPK<sub>4</sub> was removed by washing three times with medium, and the cells were incubated with liposomes containing 1 mol % CPE<sub>4</sub> decorated liposomes for 15 min. In parallel cells were incubated with liposomes in the absence of lipopeptides. After these treatments, fresh medium was added to each well, and the plate was incubated at 37 °C for 24 h prior to the WST assay. After 24 h, medium was removed and 200 μL of cell proliferation reagent WST-1 (Serva, #140330 and PMS-Ome Santa Cruz Biotechnology, #D3013) in DMEM (w/o phenol red) was added to each well, and the plate was incubated for 3 h at 37 °C. After 3 h the absorbance at 450 nm was measured at room temperature using a Tecan infinite M1000 and a 96-well plate, which was shaken for 60 s prior to measurement (2 mm linearly, 654 rpm). The values for metabolic activity (cell survival) were normalized with respect to control (no liposomes), which was set at 100% cell survival.

For the DOX cell viability assay, HeLa cells were incubated with CPK<sub>4</sub> for 2 h and then treated with series of diluted CPE decorated liposomes loaded with DOX (stock lipid concen-

tration was 1 mM, containing 1 mol % of CPE; DOX concentration was 0.25 mM), final concentration of DOX in liposomes were from 100  $\mu$ M to 0.1 nM (100  $\mu$ M, 50  $\mu$ M, 25  $\mu$ M, 10  $\mu$ M, 5  $\mu$ M, 2.5  $\mu$ M, 1  $\mu$ M, 0.1  $\mu$ M, 0.05  $\mu$ M, 0.01  $\mu$ M, 1 nM, 0.5 nM, 0.1 nM). In parallel cells were incubated with liposomes in the absence of lipopeptides. After 12 h, all the medium was removed from the wells, and cells were incubated in fresh medium for 24 h prior to the WST assay.

**Flow Cytometry Measurements.** HeLa cells and NIH/3T3 cells were seeded in a 24-well plate at a density of  $1 \times 10^5$  cells per well and incubated at 37 °C. After 21 h medium was removed and cells were incubated with 500  $\mu$ L of nocodazole (40  $\mu$ M), wortmannin (0.25  $\mu$ M), chlorpromazine (40  $\mu$ M), genistein (200  $\mu$ M), or sodium azide 0.01% w/v in medium. After 1 h preincubation, inhibitors were removed, and the cells were treated with 500  $\mu$ L of CPK<sub>4</sub> 5 ( $\mu$ M) for 2 h followed by addition of 500  $\mu$ L of CPE<sub>4</sub>-liposomes containing PI (250  $\mu$ M) in the presence of fresh inhibitors. After 15 min liposomes and inhibitors were removed and washing steps were performed. The cells were incubated at 37 °C for 1 h. Finally the cells were detached using PBS/EDTA for 15 min, centrifuged, and resuspended in fresh medium at a concentration of 200,000 cells/mL medium. The mean fluorescence intensity of the cells was measured by flow cytometry using a Beckman Coulter Quanta SC machine.

**Zebrafish Embryo Assay.** Zebrafish (*Danio rerio*) were handled in compliance with the local animal welfare regulations and maintained according to standard protocols (<http://ZF.IN.org>). Embryos were treated with 0.16 mM 1-phenyl-2-thiourea from 24 h post fertilization (hpf) to prevent pigment formation. At 48 hpf, embryos were exposed in groups of 10 in 12-well plates to 5  $\mu$ M CPK at 31 °C for 30 min; untreated embryos were used as controls. Next, embryos were washed and treated for 30 min with liposomes containing CPE, NBD-PE and DOX or PI (15  $\mu$ M). Liposomes without CPE, or liposomes without PI or DOX, or with free PI or DOX added to the medium, were used as controls. After 3 $\times$  washing in embryo medium, embryos were anesthetized in 0.02% tricaine methanesulfonate, mounted in 0.4% agarose, and imaged by confocal microscopy.

## ■ ASSOCIATED CONTENT

### 📄 Supporting Information

The Supporting Information is available free of charge on the ACS Publications website at DOI: [10.1021/acscentsci.6b00172](https://doi.org/10.1021/acscentsci.6b00172).

Full details of the methods (PDF)

## ■ AUTHOR INFORMATION

### Corresponding Authors

\*(A.K.) E-mail: [a.kros@chem.leidenuniv.nl](mailto:a.kros@chem.leidenuniv.nl).

\*(R.C.L.O.) E-mail: [olsthoor@lic.leidenuniv.nl](mailto:olsthoor@lic.leidenuniv.nl).

### Author Contributions

#J.Y. and A.B. contributed equally to this manuscript.

### Author Contributions

A.K. designed the study and supervised the work. J.Y., A.B., and J.B. performed biological studies and synthesized compounds. G.D. aided in peptide synthesis. J.Y., A.B., J.B., R.C.L.O., and A.K. wrote the manuscript.

### Notes

The authors declare no competing financial interest.

## ■ ACKNOWLEDGMENTS

We thank Gerda Lamers and Kirsten Martens for their help with confocal microscopy and Hans de Dulk for the assistance with NIH/3T3 cell line stock. This work was funded primarily through a CSC scholarship (to J.Y.), the STW VENI fellowship (No. 12520), which is financed by The Netherlands Organization for Scientific Research (NWO) (to J.B.), the European Research Council via an ERC starting grant (Contract 240391) and an ERC Proof of Concept grant (to A.B. and A.K.), and the NWO and FOM via a VICI grant (No. 724.014.001) and a programme grant (to A.K.).

## ■ REFERENCES

- (1) Conner, S. D.; Schmid, S. L. Regulated portals of entry into the cell. *Nature* **2003**, *422*, 37–44.
- (2) Sharei, A.; Zoldan, J.; Adamo, A.; Sim, W. Y.; Cho, N.; Jackson, E.; Mao, S.; Schneider, S.; Han, M. J.; Lytton-Jean, A.; Basto, P. A.; Jhunjhunwala, S.; Lee, J.; Heller, D. A.; Kang, J. W.; Hartoularos, G. C.; Kim, K. S.; Anderson, D. G.; Langer, R.; Jensen, K. F. A vector-free microfluidic platform for intracellular delivery. *Proc. Natl. Acad. Sci. U. S. A.* **2013**, *110*, 2082–2087.
- (3) Wittrup, A.; Ai, A.; Liu, X.; Hamar, P.; Trifonova, R.; Charisse, K.; Manoharan, M.; Kirchhausen, T.; Lieberman, J. Visualizing lipid-formulated siRNA release from endosomes and target gene knock-down. *Nat. Biotechnol.* **2015**, *33*, 870–876.
- (4) Nel, A. E.; Madler, L.; Velegol, D.; Xia, T.; Hoek, E. M. V.; Somasundaran, P.; Klaessig, F.; Castranova, V.; Thompson, M. Understanding biophysicochemical interactions at the nano-bio interface. *Nat. Mater.* **2009**, *8*, 543–557.
- (5) Vasir, J. K.; Labhasetwar, V. Biodegradable nanoparticles for cytosolic delivery of therapeutics. *Adv. Drug Delivery Rev.* **2007**, *59*, 718–728.
- (6) Brock, R. The uptake of arginine-rich cell-penetrating peptides: putting the puzzle together. *Bioconjugate Chem.* **2014**, *25*, 863–868.
- (7) Tunnemann, G.; Martin, R. M.; Haupt, S.; Patsch, C.; Edenhofer, F.; Cardoso, M. C. Cargo-dependent mode of uptake and bioavailability of TAT-containing proteins and peptides in living cells. *FASEB J.* **2006**, *20*, 1775–1784.
- (8) Karagiannis, E. D.; Urbanska, A. M.; Sahay, G.; Pelet, J. M.; Jhunjhunwala, S.; Langer, R.; Anderson, D. G. Rational design of a biomimetic cell penetrating peptide library. *ACS Nano* **2013**, *7*, 8616–8626.
- (9) Torchilin, V. P.; Rammohan, R.; Weissig, V.; Levchenko, T. S. TAT peptide on the surface of liposomes affords their efficient intracellular delivery even at low temperature and in the presence of metabolic inhibitors. *Proc. Natl. Acad. Sci. U. S. A.* **2001**, *98*, 8786–8791.
- (10) Nayak, S.; Herzog, R. W. Progress and prospects: immune responses to viral vectors. *Gene Ther.* **2010**, *17*, 295–304.
- (11) Wells, D. J. Gene therapy progress and prospects: Electroporation and other physical methods. *Gene Ther.* **2004**, *11*, 1363–1369.
- (12) Boukany, P. E.; Morss, A.; Liao, W. C.; Henslee, B.; Jung, H. C.; Zhang, X. L.; Yu, B.; Wang, X. M.; Wu, Y.; Li, L.; Gao, K. L.; Hu, X.; Zhao, X.; Hemminger, O.; Lu, W.; Lafyatis, G. P.; Lee, L. J. Nanochannel electroporation delivers precise amounts of biomolecules into living cells. *Nat. Nanotechnol.* **2011**, *6*, 747–754.
- (13) Chen, Y. A.; Scheller, R. H. Snare-mediated membrane fusion. *Nat. Rev. Mol. Cell Biol.* **2001**, *2*, 98–106.
- (14) Chernomordik, L. V.; Kozlov, M. M. Mechanics of membrane fusion. *Nat. Struct. Mol. Biol.* **2008**, *15*, 675–683.
- (15) Zhou, P.; Bacaj, T.; Yang, X. F.; Pang, Z. P. P.; Sudhof, T. C. Lipid-anchored SNAREs lacking transmembrane regions fully support membrane fusion during neurotransmitter release. *Neuron* **2013**, *80*, 470–483.
- (16) Jahn, R.; Lang, T.; Südhof, T. C. Membrane fusion. *Cell* **2003**, *112*, 519–533.



- (17) Jahn, R.; Scheller, R. H. SNAREs - engines for membrane fusion. *Nat. Rev. Mol. Cell Biol.* **2006**, *7*, 631–643.
- (18) Sudhof, T. C. Neurotransmitter release: the last millisecond in the life of a synaptic vesicle. *Neuron* **2013**, *80*, 675–690.
- (19) Ma, M.; Bong, D. Controlled fusion of synthetic lipid membrane vesicles. *Acc. Chem. Res.* **2013**, *46*, 2988–2997.
- (20) Pahler, G.; Panse, C.; Diederichsen, U.; Janshoff, A. Coiled-coil formation on lipid bilayers-implications for docking and fusion efficiency. *Biophys. J.* **2012**, *103*, 2295–2303.
- (21) Kumar, P.; Guha, S.; Diederichsen, U. SNARE protein analog-mediated membrane fusion. *J. Pept. Sci.* **2015**, *21*, 621–629.
- (22) Voskuhl, J.; Ravoo, B. J. Molecular recognition of bilayer vesicles. *Chem. Soc. Rev.* **2009**, *38*, 495–505.
- (23) Zope, H. R.; Versluis, F.; Ordas, A.; Voskuhl, J.; Spaink, H. P.; Kros, A. In vitro and in vivo supramolecular modification of biomembranes using a lipidated coiled-coil motif. *Angew. Chem., Int. Ed.* **2013**, *52*, 14247–14251.
- (24) Robson Marsden, H.; Elbers, N. A.; Bomans, P. H. H.; Sommerdijk, N. A. J. M.; Kros, A. A reduced SNARE model for membrane fusion. *Angew. Chem., Int. Ed.* **2009**, *48*, 2330–2333.
- (25) Robson Marsden, H.; Korobko, A. V.; Zheng, T. T.; Voskuhl, J.; Kros, A. Controlled liposome fusion mediated by SNARE protein mimics. *Biomater. Sci.* **2013**, *1*, 1046–1054.
- (26) Zheng, T.; Voskuhl, J.; Versluis, F.; Zope, H. R.; Tomatsu, I.; Marsden, H. R.; Kros, A. Controlling the rate of coiled coil driven membrane fusion. *Chem. Commun. (Cambridge, U. K.)* **2013**, *49*, 3649–3651.
- (27) Rabe, M.; Zope, H. R.; Kros, A. Interplay between lipid interaction and homo-coiling of membrane-tethered coiled-coil peptides. *Langmuir* **2015**, *31*, 9953–9964.
- (28) Rabe, M.; Schwieger, C.; Zope, H. R.; Versluis, F.; Kros, A. Membrane interactions of fusogenic coiled-coil peptides: implications for lipopeptide mediated vesicle fusion. *Langmuir* **2014**, *30*, 7724–7735.
- (29) McMahon, H. T.; Kozlov, M. M.; Martens, S. Membrane Curvature in Synaptic Vesicle Fusion and Beyond. *Cell* **2010**, *140*, 601–605.
- (30) Micka, B.; Trojanek, B.; Niemitz, S.; Lefterova, P.; Kruopis, S.; Huhn, D.; Wittig, B.; Schadendorf, D.; Schmidt-Wolf, I. G. Comparison of non-viral transfection methods in melanoma cell primary cultures. *Cytokine+* **2000**, *12*, 828–833.
- (31) Nowak, J.; Cohen, E. P.; Graf, L. H., Jr. Cytotoxic activity toward mouse melanoma following immunization of mice with transfected cells expressing a human melanoma-associated antigen. *Cancer Immunol. Immunother.* **1991**, *33*, 91–96.
- (32) Pang, W. J.; Xiong, Y.; Wang, Y.; Tong, Q.; Yang, G. S. SirT1 attenuates camptothecin-induced apoptosis through caspase-3 pathway in porcine preadipocytes. *Exp. Cell Res.* **2013**, *319*, 670–683.
- (33) Singal, P. K.; Iliskovic, N. Doxorubicin-induced cardiomyopathy. *N. Engl. J. Med.* **1998**, *339*, 900–905.
- (34) Arcaro, A.; Wymann, M. P. Wortmannin is a potent phosphatidylinositol 3-kinase inhibitor: the role of phosphatidylinositol 3,4,5-trisphosphate in neutrophil responses. *Biochem. J.* **1993**, *296*, 297–301.
- (35) Araki, N.; Johnson, M. T.; Swanson, J. A. A role for phosphoinositide 3-kinase in the completion of macropinocytosis and phagocytosis by macrophages. *J. Cell Biol.* **1996**, *135*, 1249–1260.
- (36) Payne, C. K.; Jones, S. A.; Chen, C.; Zhuang, X. Internalization and trafficking of cell surface proteoglycans and proteoglycan-binding ligands. *Traffic (Oxford, U. K.)* **2007**, *8*, 389–401.
- (37) Coppola, S.; Estrada, L. C.; Digman, M. A.; Pozzi, D.; Cardarelli, F.; Gratton, E.; Caracciolo, G. Intracellular trafficking of cationic liposome-DNA complexes in living cells. *Soft Matter* **2012**, *8*, 7919–7927.
- (38) Wang, L. H.; Rothberg, K. G.; Anderson, R. G. Mis-assembly of clathrin lattices on endosomes reveals a regulatory switch for coated pit formation. *J. Cell Biol.* **1993**, *123*, 1107–1117.
- (39) von Gersdorff, K.; Sanders, N. N.; Vandenbroucke, R.; De Smedt, S. C.; Wagner, E.; Ogris, M. The internalization route resulting in successful gene expression depends on both cell line and polyethylenimine polyplex type. *Mol. Ther.* **2006**, *14*, 745–753.
- (40) Huth, U. S.; Schubert, R.; Peschka-Suss, R. Investigating the uptake and intracellular fate of pH-sensitive liposomes by flow cytometry and spectral bio-imaging. *J. Controlled Release* **2006**, *110*, 490–504.
- (41) Gabrielson, N. P.; Pack, D. W. Efficient polyethylenimine-mediated gene delivery proceeds via a caveolar pathway in HeLa cells. *J. Controlled Release* **2009**, *136*, 54–61.
- (42) Akiyama, T.; Ishida, J.; Nakagawa, S.; Ogawara, H.; Watanabe, S.; Itoh, N.; Shibuya, M.; Fukami, Y. Genistein, a specific inhibitor of tyrosine-specific protein kinases. *J. Biol. Chem.* **1987**, *262*, 5592–5595.
- (43) Orlandi, P. A.; Fishman, P. H. Filipin-dependent inhibition of cholera toxin: evidence for toxin internalization and activation through caveolae-like domains. *J. Cell Biol.* **1998**, *141*, 905–915.
- (44) Rejman, J.; Oberle, V.; Zuhorn, I. S.; Hoekstra, D. Size-dependent internalization of particles via the pathways of clathrin- and caveolae-mediated endocytosis. *Biochem. J.* **2004**, *377*, 159–169.
- (45) Goncalves, C.; Mennesson, E.; Fuchs, R.; Gorvel, J. P.; Midoux, P.; Pichon, C. Macropinocytosis of polyplexes and recycling of plasmid via the clathrin-dependent pathway impair the transfection efficiency of human hepatocarcinoma cells. *Mol. Ther.* **2004**, *10*, 373–385.
- (46) Simoes, S.; Slepishkin, V.; Duzgunes, N.; Pedroso de Lima, M. C. On the mechanisms of internalization and intracellular delivery mediated by pH-sensitive liposomes. *Biochim. Biophys. Acta, Biomembr.* **2001**, *1515*, 23–37.
- (47) Gao, H.; Yang, Z.; Zhang, S.; Cao, S.; Shen, S.; Pang, Z.; Jiang, X. Ligand modified nanoparticles increases cell uptake, alters endocytosis and elevates glioma distribution and internalization. *Sci. Rep.* **2013**, *3*, 2534.
- (48) Szoka, F.; Magnusson, K. E.; Wojcieszyn, J.; Hou, Y.; Derzko, Z.; Jacobson, K. Use of lectins and polyethylene glycol for fusion of glycolipid-containing liposomes with eukaryotic cells. *Proc. Natl. Acad. Sci. U. S. A.* **1981**, *78*, 1685–1689.
- (49) Mora, N. L.; Bahreman, A.; Valkenier, H.; Li, H. Y.; Sharp, T. H.; Sheppard, D. N.; Davis, A. P.; Kros, A. Targeted anion transporter delivery by coiled-coil driven membrane fusion. *Chem. Sci.* **2016**, *7*, 1768–1772.
- (50) Oude Blenke, E. E.; van den Dikkenberg, J.; van Kolck, B.; Kros, A.; Mastrobattista, E. Coiled coil interactions for the targeting of liposomes for nucleic acid delivery. *Nanoscale* **2016**, *8*, 8955–8965.
- (51) Kanasty, R.; Dorkin, J. R.; Vegas, A.; Anderson, D. Delivery materials for siRNA therapeutics. *Nat. Mater.* **2013**, *12*, 967–977.
- (52) Wittrup, A.; Ai, A.; Liu, X.; Hamar, P.; Trifonova, R.; Charisse, K.; Manoharan, M.; Kirchhausen, T.; Lieberman, J. Visualizing lipid-formulated siRNA release from endosomes and target gene knock-down. *Nat. Biotechnol.* **2015**, *33*, 870.
- (53) Liu, J. W.; Jiang, X. M.; Ashley, C.; Brinker, C. J. Electrostatically mediated liposome fusion and lipid exchange with a nanoparticle-supported bilayer for control of surface charge, drug containment, and delivery. *J. Am. Chem. Soc.* **2009**, *131*, 7567–7569.
- (54) Liu, J. W.; Stace-Naughton, A.; Jiang, X. M.; Brinker, C. J. Porous nanoparticle supported lipid bilayers (protocells) as delivery vehicles. *J. Am. Chem. Soc.* **2009**, *131*, 1354–1355.
- (55) Ashley, C. E.; Carnes, E. C.; Epler, K. E.; Padilla, D. P.; Phillips, G. K.; Castillo, R. E.; Wilkinson, D. C.; Wilkinson, B. S.; Burgard, C. A.; Kalinich, R. M.; Townson, J. L.; Chackerian, B.; Willman, C. L.; Peabody, D. S.; Wharton, W.; Brinker, C. J. Delivery of small interfering RNA by peptide-targeted mesoporous silica nanoparticle-supported lipid bilayers. *ACS Nano* **2012**, *6*, 2174–2188.
- (56) Liu, X. S.; Situ, A.; Kang, Y. A.; Villabroza, K. R.; Liao, Y. P.; Chang, C. H.; Donahue, T.; Nel, A. E.; Meng, H. Irinotecan delivery by lipid-coated mesoporous silica nanoparticles shows improved efficacy and safety over liposomes for pancreatic cancer. *ACS Nano* **2016**, *10*, 2702–2715.
- (57) Cauda, V.; Engelke, H.; Sauer, A.; Arcizet, D.; Brauchle, C.; Radler, J.; Bein, T. Colchicine-loaded lipid bilayer-coated 50 nm mesoporous nanoparticles efficiently induce microtubule depolymerization upon cell uptake. *Nano Lett.* **2010**, *10*, 2484–2492.

(58) Wang, K.; Huang, Q.; Qiu, F.; Sui, M. Non-viral delivery systems for the application in p53 cancer gene therapy. *Curr. Med. Chem.* **2015**, *22*, 4118–4136.

(59) Saito, Y.; Nakaoka, T.; Saito, H. MicroRNA-34a as a therapeutic agent against human cancer. *J. Clin. Med.* **2015**, *4*, 1951–1959.

(60) Kong, L.; Askes, S. H.; Bonnet, S.; Kros, A.; Campbell, F. Temporal control of membrane fusion through photolabile PEGylation of liposome membranes. *Angew. Chem., Int. Ed.* **2016**, *55*, 1396–1400.

(61) Voskuhl, J.; Wendeln, C.; Versluis, F.; Fritz, E. C.; Roling, O.; Zope, H.; Schulz, C.; Rinnen, S.; Arlinghaus, H. F.; Ravoo, B. J.; Kros, A. Immobilization of liposomes and vesicles on patterned surfaces by a peptide coiled-coil binding motif. *Angew. Chem., Int. Ed.* **2012**, *51*, 12616–12620.

(62) Sun, Q.; Cai, S.; Peterson, B. R. Practical synthesis of 3beta-amino-5-cholestene and related 3beta-halides involving i-steroid and retro-i-steroid rearrangements. *Org. Lett.* **2009**, *11*, 567–570.